H. B. Papo
E. Gelbman
Department of Civil Engineering
Technion, Haifa, Israel

Digital Terrain Models for Slopes and Curvatures

Slopes and curvatures of the terrain are derived from the two-dimensional Fourier Transform of the conventional DTM.

Introduction

The conventional, regular (equally spaced) digital terrain model (DTM) is well established as an effective discrete representation of the terrain. With the advent of digital computers and automatic plotters, it has become the primary data source for a wide range of graphical products. There are, however, certain applications associated with terrain analysis for which the conventional DTM is not necessarily the best data source. A more efficient form for storage and subsequent usage of the data, one which provides, in addition, for a better insight into the terrain's geometrical characteristics, is the two-dimensional Fourier Transform (DTM-G) of the conventional DTM-Z.

With the Fourier Transform DTM-G as the data source, we propose a number of computational modules for the following purposes:

- Reproduce a conventional DTM-Z (elevations) with or without intermediate smoothing,
- Use the DTM-G directly in certain aspects of qualitative and quantitative terrain analysis, or
- Derive first and second derivatives of the terrain which are transformed subsequently into DTM for slopes and curvatures.

The use of terrain models for slopes and curvatures in a digital or in a graphical form may be unpopular at present, but it is mostly a matter of availability and of education. Users have been forced to develop intuitive and not too precise ways of assessing slopes and curvatures directly from the conventional graphical data forms (contour line maps). Potential areas of application of the proposed DTM forms can be found in civil, military, agricultural, and aeronautical engineering in addition to the mapping sciences.

Abstract: *The concept of the conventional DTM (elevations) as the sole numerical descriptor of topography is extended to include DTM of slopes and curvatures. There are numerous areas of application where direct and efficient use can be made of those new forms of DTM. The transformation from DTM for elevations into DTM for slopes and curvatures is based on the well known and highly efficient Fast Fourier Transform algorithm. The bulk of calculations can be performed on a large size computer or on a microcomputer. An example which illustrates the proposed procedure is given in the paper.*

Two-Dimensional Fourier Transform of the Terrain

The terrain function, Z, in its discrete representation, i.e., the Digital Terrain Model (DTM-Z), describes the terrain surface in a position-oriented manner. The elevation (Z) of a point is defined as a function of its position (X and Y coordinates). Using conventional mathematical terminology, we could say that the DTM-Z represents the terrain in the space domain (Bath, 1974, p. 12). The terrain could be represented also in the spatial-frequency domain where Z is defined as the sum of a set of surface harmonics. Direct and inverse transformation from the space domain (DTM-Z) to spatial-frequency domain (DTM-G) representation of the terrain is obtained using the discrete Fourier transform algorithm. On a digital computer the direct and inverse discrete Fourier transforms are performed most efficiently by the well known Fast Fourier Transform (FFT) algorithm (Bath, 1974; Brigham, 1974). The rest of this section contains a short formulation of the direct and inverse discrete Fourier transforms extended to two dimensions.

First, we discuss Z as a function of a single argument, i.e., $Z = Z(X)$. Let a profile of the terrain

Photogrammetric Engineering and Remote Sensing,
Vol. 50, No. 6, June 1984, pp. 695-701.
0099-1112/84/5006-0695$02.25/0

be represented by an ordered set of N equally spaced points with elevations Z_k where $k = 0, 1, 2, \ldots, N-1$. In the following equation Z_k is represented by the sum of N harmonics: i.e.,

$$Z_k = \frac{1}{N} \sum_{n=0}^{N-1} G_n \cdot W^{nk},$$

$$(k = 0, 1, 2, 3, \ldots, N-1) \qquad (1)$$

where $W = e^{i \cdot 2\Pi/N}$, $i = \sqrt{-1}$,
$X_k = k \cdot d$, d is the regular interval, and
G_n is the amplitude of the n^{th} harmonic.

The wave-length of the n^{th} harmonic is equal to the $(N-n)^{\text{th}}$: i.e.,

$$\omega_n = \frac{N \cdot d}{n}; \quad \omega_n = \frac{N \cdot d}{N-n}$$

$$0 < n \leq N/2 \quad N/2 \leq n < N$$

Equation 1 is the inverse discrete Fourier transform, whereas the direct transform is

$$G_n = \sum_{k=0}^{N-1} Z_k \cdot W^{-nk}, \ (n = 0, 1, 2, \ldots, N-1) \qquad (2)$$

The direct and inverse Fourier transforms for a two-dimensional terrain function $Z(X,Y)$ are similar to the above. Assume a regular DTM-Z, i.e., a matrix of N by M Z_{kl} elevations which represents discretely a given terrain. Then direct transform is

$$G_{nm} = \sum_{l=0}^{M-1} \sum_{k=0}^{N-1} Z_{kl} \cdot W_N^{-nk} \cdot W_M^{-ml},$$

$$(n = 0, 1, 2, 3, \ldots, N-1),$$
$$(m = 0, 1, 2, 3, \ldots, M-1); \qquad (3)$$

and inverse transform is

$$Z_{kl} = \frac{1}{N \cdot M} \sum_{n=0}^{N-1} \sum_{m=0}^{M-1} G_{nm} \cdot W_N^{nk} \cdot W_M^{ml},$$

$$(k = 0, 1, 2, 3, \ldots, N-1),$$
$$(l = 0, 1, 2, 3, \ldots, M-1), \qquad (4)$$

where $W_N = e^{i \cdot 2\Pi/N}$ and $W_M = e^{i \cdot 2\Pi/M}$.

The algorithm for performing two-dimensional Fourier transforms is based on a sequential application of the one-dimensional FT: first in one direction (for example, X) and then in the other direction (Y). Equation 3 can be rewritten as follows:

$$G_{nm} = \sum_{l=0}^{M-1} Q_l \cdot W_M^{-ml} \qquad (3')$$

where

$$Q_l = \sum_{k=0}^{N-1} Z_{kl} \cdot W_N^{-nk}.$$

The G_{nm} coefficients (including real and imaginary components), arranged by their n and m subscripts, are the spatial frequency domain representation of the terrain, denoted by us as the DTM-G. Another useful derivative of the DTM-G is the power spectrum of the terrain, which is an N by M matrix containing the modules of the complex G_{nm} coefficients.

Figure 1 shows a perspective block diagram of a hilly terrain in northern Israel. The 2.5 by 5.0 km regular DTM-Z of that terrain was measured on a Wild A-7 Autograph equipped with encoders and a diskette drive. The sampling density ($d_x = d_y = 40$ m) was high as related to the average roughness of the terrain, which enabled us to experiment with various degrees of low-pass filters (suppression of high frequencies in the original DTM-G).

Figure 2 shows a perspective view of the two-dimensional power spectrum of the same terrain. Note the following characteristics of the power spectrum of the terrain:

- symmetry with respect to the center (highest frequency) harmonic: $n = N/2$ and $m = M/2$,
- over all flatness in the high frequencies, and
- the low-pass-filter depression rectangle.

The low-pass-filtered DTM-G served subsequently as a data base for a number of experiments, which are reported upon in a later section of this paper.

First and Second Derivatives of the Terrain

The fundamental geometric properties which characterize the terrain surface at a point are its elevation, slope, and some measure of its curvature. The slope and curvature at a point are associated with the first and second derivatives of the terrain function $Z = Z(X,Y)$. Using differential geometry formalism, we can evaluate the components of the gradient vector or its magnitude and direction angle (s and g). The curvature at a point can be defined by the principal radii of curvature of the surface or by their function. The first order derivatives $\partial Z/\partial X$ and $\partial Z/\partial Y$ are related directly to the slope at a point as follows:

$s = \sqrt{(\partial Z/\partial X)^2 + (\partial Z/\partial Y)^2}$ is the slope's magnitude and $\qquad (5)$

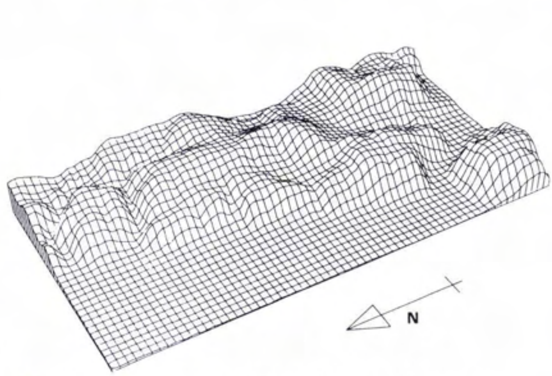

Fig. 1. A perspective block diagram of the terrain.

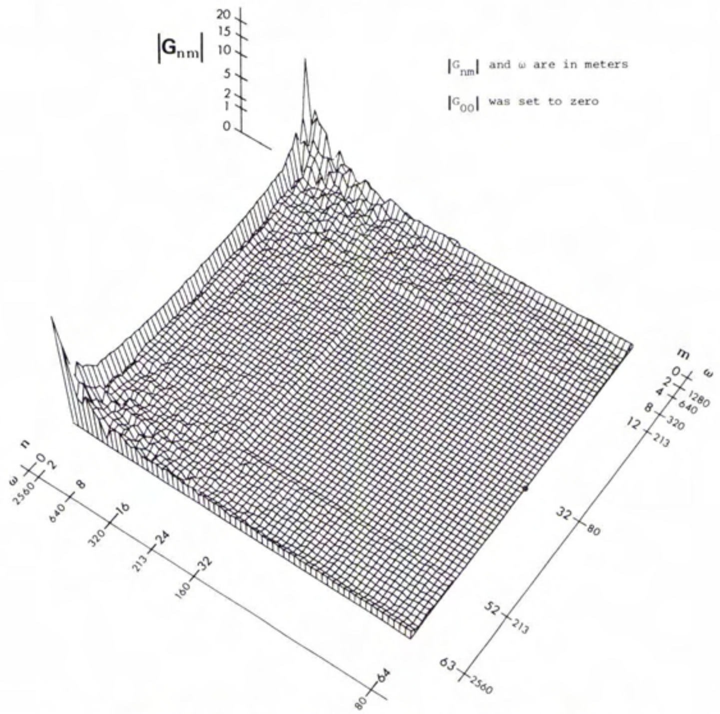

Fig. 2. Power spectrum of the terrain—a perspective view.

$$g = \arctan\left(\frac{\partial Z/\partial Y}{\partial Z/\partial X}\right) \text{ is the slope's direction angle.}$$

The curvature at a point is evaluated by more complicated expressions, which are in general functions of the second order derivatives $\partial^2 Z/\partial X^2$, $\partial^2 Z/\partial X \partial Y$ and $\partial^2 Z/\partial Y^2$ as follows:

$$C_M = \frac{1}{R_1} + \frac{1}{R_2} = \frac{E \cdot D'' + G \cdot D - 2F \cdot D'}{E \cdot G - F^2}$$

$$C_T = \frac{1}{R_1 \cdot R_2} = \frac{D \cdot D'' - D'^2}{E \cdot G - F^2} \tag{6}$$

where

C_M and C_T are the mean and total curvatures of the surface, respectively;
R_1 and R_2 are the principal radii of curvature; and
E, F, G and D, D', D'' are the respective first- and second-order fundamental quantities of the surface (Thomas, 1952, p. 49).

Another measure for the curvature of the surface which is much easier to evaluate is the Laplacian (c):

$$c = \partial^2 Z/\partial X^2 + \partial^2 Z/\partial Y^2 \tag{7}$$

The difference between c and C_M is a function of the first-order derivatives (see Gelbman (1981) for a detailed derivation), and for terrain with slopes of up to 40 percent ($s \leq 0.4$) the difference is smaller than 4 percent. Thus, in order to evaluate the s, g, and c quantities at a point, we need two first- and two second-order derivatives of the terrain at that point.

We selected the "moving surface" approach as a basis for finite element differentiation of the DTM-Z grid. First, we fit a second- or a third-degree polynomial $z = z(x,y)$ over a subset of the DTM-Z. The subset is composed of 9 = 3 by 3 or of 25 = 5 by 5 grid points including at its center the object (k,l) point (see Figure 3).

The general form of such a polynomial is

$$z_u = z_u\,(x,y) = \sum_{q=0}^{u} \sum_{p=0}^{u-q} a_{pq} \cdot x^p \cdot y^q \tag{8}$$

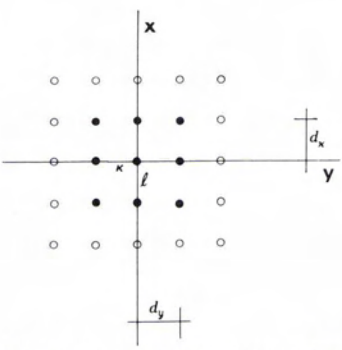

Fig. 3. A nine-point DTM-Z subset.

where u is the degree of the polynomial (the total number of coefficients a_{pq} being $(u + 1) \cdot (u + 2)/2$) and x,y are the Cartesian coordinates of a point in the subset with respect to the (k,l) point. The derivatives of z are obtained in a straightforward manner where, for example, for $u = 2$ we have

$$\partial z/\partial x = a_{10} + a_{11} \cdot y + 2a_{20} \cdot x \tag{9}$$

The expressions for the derivatives are greatly simplified because of selecting the origin of the xy system at the (k,l) point. As a result, we obtain the following expressions for s, g, and c:

$$\begin{aligned} s &= \sqrt{a_{10}^2 + a_{01}^2} \\ g &= \arctan\,(a_{01}/a_{10}) \\ c &= 2\,(a_{20} + a_{02}) \end{aligned} \tag{10}$$

The results of the least-squares fit of the Equation 8 polynomial are a_{pq} coefficients which are linear functions of the 9- or 25-point subset Z values. For example, for $u = 2$ and a 9-point subset we obtain

$$a_{10(k,l)} = \frac{1}{6d} \sum_{j=l-1}^{l+1} (Z_{k+1,j} - Z_{k-1,j}). \tag{11}$$

At this stage we substitute for $Z_{k+1,l-1}, Z_{k+1,l}$, etc. in Equation 11 above their equivalents (their inverse Fourier transforms) as taken from Equation 4. Through laborious and patient algebra we arrive finally at the following general expressions for a_{10}, a_{01}, and c:

$$[a_{10}\; a_{01}\; c]_{(k,l)} = \frac{1}{v \cdot d \cdot M \cdot N} \sum_{n=0}^{N-1} \sum_{m=0}^{M-1} \{G_{nm} \cdot W_N^{nk} \cdot W_M^{ml} \cdot [f_{10}\, f_{01}\, f_c]_{(n,m)}\} \tag{12}$$

where v and f_{10}, f_{01}, and f_c are coefficients which are independent of k and l. For the above example of $u = 2$ and a 9-point subset, we obtain the following expressions:

$$f_{10\,(n,m)} = (W_N^n - W_N^{-n}) \cdot [1 + (W_M^m + W_M^{-m})] \tag{13}$$

$$f_{01\,(n,m)} = (W_M^m - W_M^{-m}) \cdot [1 + (W_N^n + W_N^{-n})] \tag{14}$$

$$\begin{aligned} f_{c\,(n,m)} = 2\,[&2\,(W_N^n - W_N^{-n}) \cdot (W_M^m - W_M^{-m}) \\ &-(W_N^n + W_N^{-n}) - (W_M^m + W_M^{-m}) - 4] \end{aligned} \tag{15}$$

We can see that the evaluation of a_{01} a_{10} and c in Equation 12 is similar in form to the ordinary inverse Fourier transform as shown in Equation 4. The two-dimensional FFT algorithm is applied to the spectral density matrix DTM-G where each G_{nm} element is premultiplied by the appropriate (nm) coefficient: i.e., 1, f_{01}, f_{10}, or f_c. The expressions for evaluating s and g (Equation 10) conclude the computational process. Thus, we have generated four digital models which completely describe the terrain. Using the spectral density model DTM-G as a data source, we can produce elevation (DTM-Z), slope (DTM-s/g), and curvature (DTM-c) digital models of the terrain.

We should point out that most of the above transforms are performed in parallel for a considerable savings in time (CPU). This is made possible by the particular properties of the Fourier transforms as well as due to the fact that the DTM-Z, DTM-c, and DTM-g,s are composed of complex numbers with zero imaginary components.

Experiments

As a natural conclusion of the study reported in the previous sections, a package of computer programs was prepared to perform all the necessary operations for the generation, storage, print-out, and graphical display of the new forms of DTM.

Figure 4 shows a schematic flowchart of the software package. The rectangles represent the various forms of the data while the ellipses represent the program modules. The intervention of the operator is required at almost every step (ellipse) of the flowchart. The various DTM's are accompanied by accuracy estimates (σ) which are derived from the *a-priori* σ_Z following its propagation through the intermediate mathematical operations. The DTM's affected by the smoothing operation are marked with overbars.

The DTM-G of the 2.5 by 5.0 km terrain block mentioned in the second part of this paper was subjected to smoothing. Smoothing was produced by applying a low-pass filter on the DTM-G matrix: i.e., the G_{nm} coefficients corresponding to wavelengths shorter than 213 m were set to zero ($24 < n < 104$;

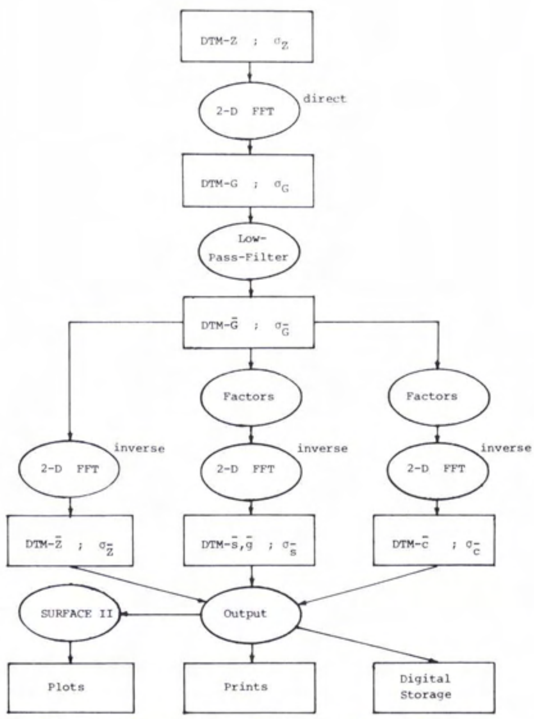

FIG. 4. Schematic flowchart of terrain data forms.

$12 < m < 52$; see also figure 2). As a result of smoothing, the total number of coefficients in DTM-G was reduced by 40 percent. The difference between the contour-line maps before and after smoothing was negligible and was considered well within the accuracy bounds of the original DTM-Z.

There are many ways for representing, digitally and graphically, DTM's of slopes and curvatures. Of the many different experiments we did, we have chosen to present in this paper only a few which did appeal to our "topographical" sense. All those representations are made with the contour-line map of the terrain as a background. The reader can use the background contours in order to check his intuitive perception of slopes and curvatures against what the computer had to say.

Figure 5 shows a "hachured" slope map of the terrain, where the arrows point downhill (direction of steepest descent) and their length is proportional to the module of the gradient (s). The middle of each arrow on the map corresponds to the position of the respective node.

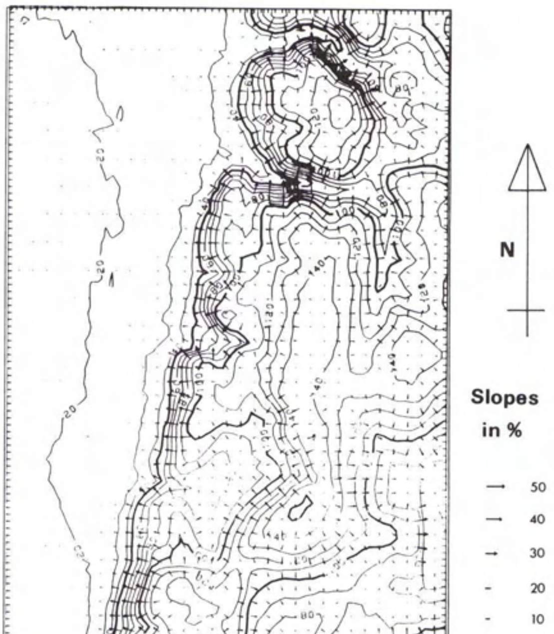

FIG. 5. Arrows slope map of the terrain.

Plate 1 is another graphical representation of the DTM of slopes. It can be characterized as a tinted or a layered slope map. Darker shades correspond to steeper slopes and, vice-versa, blank areas stand for level terrain (slopes below the 15 percent limit). In both slope maps, features of interest are the narrow wadies in the northern part as well as the ubrupt ascent of the topography from the flat and low coastal plain (western part of the map) towards the high and undulating hills of the eastern part.

Plate 2 is similar in appearance to Plate 1, only it represents curvatures. The three levels of brown stand for upwardly convex areas while the three levels of green represent concave areas. Areas with radii of curvature greater than 286 m are shown as blank areas and constitute the major part of the map. It is interesting to note the "curvature" picture along the narrow wadies. The ubrupt rise from west to east has its own curvature signature. Note also the curved borders of the wide and generally flat valley entrance on the southern part of the map.

CONCLUSIONS

Two new digital derivatives of the conventional DTM were presented, namely, the DTM of slopes and the DTM of curvatures. The new forms of DTM and the conventional DTM of elevations complement each other in providing information on the topography from different points of view.

The fast Fourier transform (FFT) algorithm, which was used to process the various data forms, has many attractive properties. In addition to the remarkable savings in computer time, it provides, through the spectral density matrix, for an excellent insight into the inherent characteristics of the topography.

Users of the new forms of DTM could come from various branches of the engineering profession. We have agricultural engineers interested in applying our programs for investigating the correlation between soil fertility and surface curvature. Construction engineers have approached us for help in investigating the surface of concrete formworks. Highway engineers could benefit from the availability of DTM-G or DTM-c of airfield runway surfaces. Military engineers could most efficiently orient themselves in unfamiliar areas with the help of appropriate slope maps. The list of potential users is undoubtedly much longer and we haven't included the mapping sciences.

ACKNOWLEDGMENTS

The support provided by the following institutions is gratefully acknowledged: Fund for the Promotion of Research at The Technion, Haifa; The Geodetic Research Station—The Technion, Haifa; and The Survey of Israel—Department of Cartography, Tel Aviv.

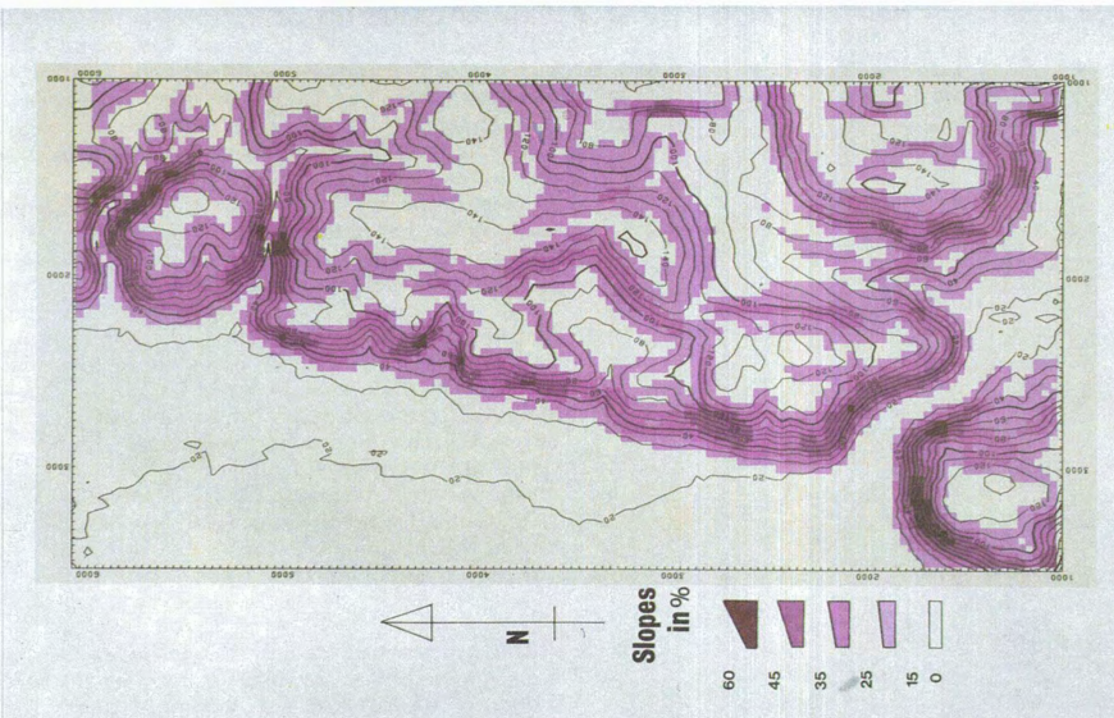

PLATE 1. Tinted zones slope map of the terrain.

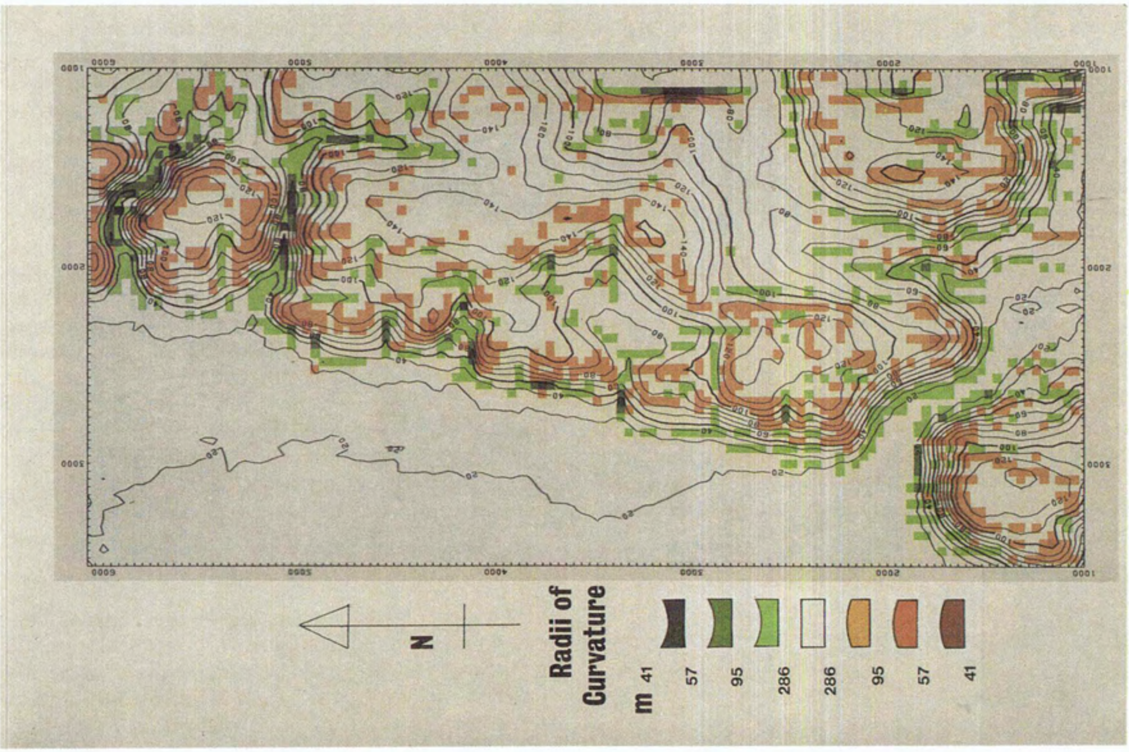

PLATE 2. Tinted zones curvature map of the terrain.

References

Bath, M., 1974. *Spectral Analysis in Geophysics*, Elsevier Scient. Publ. Co., Amsterdam.

Brigham, E. O., 1974. *The Fast Fourier Transform*, Prentice-Hall Inc., Englewood Cliffs, N.J.

Davis, J. C., 1973. *Statistics and Data Analysis in Geology*, John Wiley & Sons Inc., N.Y.

Gelbman, E., 1981. *Generalization of the DTM to Represent Slopes and Curvatures* (in Hebrew), MS Thesis, Technion, Haifa.

Ralston, A., 1965. *A First Course in Numerical Analysis*, McGraw Hill/Kogakusha Co. Ltd., N.Y., Tokyo.

Sampson, P. J., 1978. *Surface II Graphics System*, Kansas Geological Survey, Lawrence, Kansas.

Thomas, P., 1952. *Conformal Projections in Geodesy and Cartography*, U.S. Dept. of Commerce, C&GS, Special Publ. No. 251, Washington D.C.

(Received 7 February 1983; accepted 16 July 1983; revised 28 January 1984)

International Conference on Training for Remote Sensing Users

Toulouse, France
8-11 October 1984

The aim of the Conference—organized by the Groupement pour le Développement de la Télédétection Aérospatiale and sponsored by the Ministère des Relations Extérieures, the Ministère de l'Industrie et de la Recherche, the Centre National d'Etudes Spatiales, and the Conseil Régional Midi-Pyrénées—is to review the various training programs existing all over the world, to estimate the importance of educational needs, and to promote relationships between demanders and training suppliers. The conference will be divided into three parts:

- Presentation of various remote sensing training centers
- Estimation, by various international agencies, of education needs in the forthcoming year: e.g., researchers, technical staff, experts, etc.
- Discussions on the necessary development of training, taking into account the following points:
  —evolution of future systems
  —national politics
  —international cooperation
  —development projects
  —pedagogic constraints

For further information please contact

G.D.T.A. formation—Section "Colloques"
18, avenue Edouard-Belin
31055 Toulouse Cedex, France